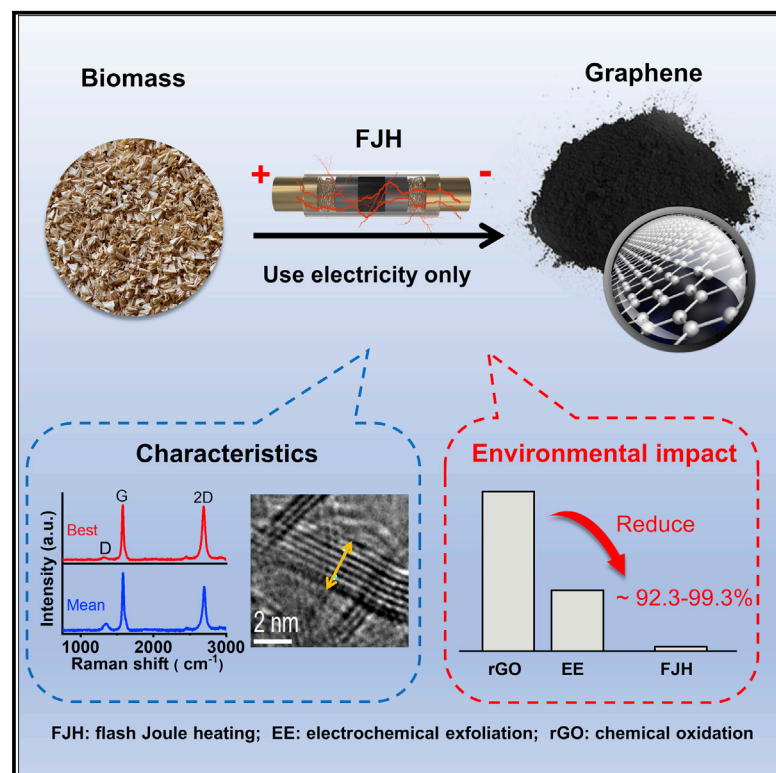


Graphene environmental footprint greatly reduced when derived from biomass waste via flash Joule heating

Graphical abstract



Authors

Chao Jia, Mingyue Pang, Yuanda Lu, ..., Yong-Guan Zhu, Xiangdong Zhu, Yi Yang

Correspondence

zxdjewett@fudan.edu.cn (X.Z.), yi.yang@cqu.edu.cn (Y.Y.)

In brief

Graphene is an important material utilized in many applications. However, the current production of graphene based on natural or artificial graphite is expensive and environmentally unfriendly. Flash Joule heating (FJH) emerges as a cleaner production process, and biomass waste could provide a more renewable feedstock, but graphene quality and the life cycle sustainability of such a process remain unclear. Here we conduct lab-scale examinations and show that FJH can produce high-quality flash graphene from biomass waste with a ~90% reduction in environmental footprint (especially carbon emissions and freshwater use) and significantly lower costs.

Highlights

- Biomass waste is converted to flash graphene (FG) via a flash Joule heating process
- The life cycle environmental impacts of biomass waste-derived FG were analyzed
- Biomass waste-enabled FG has low environmental impacts and can be carbon neutral
- FG made from biomass waste can be >10 times cheaper than regular graphene



Article

Graphene environmental footprint greatly reduced when derived from biomass waste via flash Joule heating

Chao Jia,^{1,12} Mingyue Pang,^{2,12} Yuanda Lu,¹ Yize Liu,³ Minghao Zhuang,³ Beibei Liu,⁴ Jiahao Lu,⁵ Tao Wei,⁵ Liang Wang,⁵ Ting Bian,⁵ Meiling Wang,⁶ Fengbo Yu,¹ Liming Sun,¹ Litao Lin,^{1,5} Tao Teng,¹ Xuan Wu,¹ Zhelin He,¹ Jie Gao,¹ Jiewen Luo,¹ Shicheng Zhang,^{1,7} Lei Feng,² Xinhan Yin,² Fengqi You,⁸ Gang Li,^{9,10} Lixiao Zhang,¹¹ Yong-Guan Zhu,⁹ Xiangdong Zhu,^{1,*} and Yi Yang^{2,13,*}

¹Shanghai Technical Service Platform for Pollution Control and Resource Utilization of Organic Wastes, Shanghai Key Laboratory of Atmospheric Particle Pollution and Prevention (LAP3), Department of Environmental Science and Engineering, Fudan University, Shanghai, China

²Key Laboratory of Three Gorges Reservoir Region's Eco-Environment, Ministry of Education, Chongqing University, Chongqing, China

³College of Resources and Environmental Sciences, National Academy of Agriculture Green Development, Key Laboratory of Plant-Soil Interactions, Ministry of Education, China Agricultural University, Beijing, China

⁴State Key Laboratory of Pollution Control & Resource Reuse School of Environment, Nanjing University, Nanjing, China

⁵School of Energy and Power Engineering, Jiangsu University of Science and Technology, Zhenjiang, Jiangsu, China

⁶Institute of Intelligent Machines Hefei Institutes of Physical Science, Chinese Academy of Sciences, Changzhou, China

⁷Shanghai Institute of Pollution Control and Ecological Security, Shanghai, China

⁸Robert Frederick Smith School of Chemical and Biomolecular Engineering, Cornell University, Ithaca, NY, USA

⁹Key Lab of Urban Environment and Health, Institute of Urban Environment, Chinese Academy of Sciences, Xiamen, China

¹⁰Yangtze Delta Region Healthy Agriculture Institute, Jiaxing, Zhejiang, China

¹¹State Key Joint Laboratory of Environmental Simulation and Pollution Control, School of Environment, Beijing Normal University, Beijing, China

¹²These authors contributed equally

¹³Lead contact

*Correspondence: zxdjewett@fudan.edu.cn (X.Z.), yi.yang@cqu.edu.cn (Y.Y.)

<https://doi.org/10.1016/j.oneear.2022.11.006>

SCIENCE FOR SOCIETY Graphene is a strong, flexible, and light material with impressive heat and electricity conduction properties. These characteristics have seen it dubbed as a “wonder material,” and it is revolutionizing a wide range of applications that are vital to sustainable development, from energy storage to health-care. Existing graphene production approaches are, however, unsustainable. The feedstock, or origin material, usually comes from mining graphite, and the production of graphene from graphite requires intensive use of chemical solvents and energy that have substantial environmental impacts. Flash Joule heating (FJH) has recently emerged as a cleaner graphene production process, and biomass waste (e.g., wheat straws) that has a carbon-rich structure is a potential renewable alternative to graphite. However, the sustainability credentials of the FJH approach remain unclear, and it is far from certain whether FJH can use biomass waste to produce industry-quality graphene. Our lab results show that high-quality flash graphene can be obtained from biomass waste via FJH. Importantly, the FJH process not only lessens carbon and water footprints by more than 90%, but is also much more cost effective, compared with existing technologies.

SUMMARY

Graphene is widely applied in many important technologies, with demand projected to grow exponentially. Conventional graphene production approaches that use natural/artificial graphite are expensive and energy and chemical intensive, resulting in a significant environmental footprint. The recent flash Joule heating (FJH) technology that can produce flash graphene (FG) from carbon-rich waste materials has been proposed as a cleaner production process, but the quality of FG made from biomass waste via FJH and the overall sustainability of the process remain unclear. Here we conduct lab-scale experiments to fill these knowledge gaps. We show that biomass waste-derived FG shows excellent thermal and electrical conductivity, and the FJH process results in a more than 10-fold decrease in life-cycle environmental impacts including carbon emissions and freshwater use relative to the conventional approaches. The FJH process is also cost effective, with the biomass waste-derived FG being much cheaper than graphite-based graphene. Our study identifies circular and sustainable opportunities for future graphene production.

INTRODUCTION

Over the past two decades, graphene has attracted massive attention in research, industry, and policy arenas.¹ It is the thinnest and strongest material known to mankind, with numerous unique and exceptional properties including large theoretical specific surface area,² high intrinsic mobility,³ and high thermal and electrical conductivity.⁴ This new material is expected to revolutionize a wide range of industries from biomedical, electronics, and energy storage to aerospace.^{5–8} For example, it can substantially improve the performance—including energy density, power, and safety—of electrochemical energy storage devices, and thus it may accelerate the transition to renewable energy. Many countries have proposed and implemented major fiscal stimulus plans to accelerate the industrialization and commercialization of graphene.^{9,10}

At present, the primary approaches to the bulk-scale preparation of graphene rely on a top-down synthesis: exfoliating graphene (e.g., via oxidation-reduction, liquid phase stripping, or mechanical exfoliation).^{11–14} However, these approaches face several environmental challenges. First, they require intensive use of solvents (such as H_2SO_4 and KMnO_4), sonication, or electrochemical treatment, posing potential environmental and health risks.^{15–18} Second, they are energy and carbon intensive, with a carbon footprint up to ~ 620 g CO_2 equivalent (CO_2e) per g of graphene produced.¹⁹ Third, they are highly dependent on the supply of natural graphite, which could be depleted in the next few decades if mined at 5.6% annual increments (Figure 1).^{20–22} Although graphene can be produced from artificial graphite by carbonization and graphitization of organics (such as petroleum coke), artificial graphite has much greater environmental impacts than natural graphite.^{23,24} Given these challenges, efforts have been made to seek more sustainable feedstocks, such as crop residues, waste plastics, and discarded batteries.^{25–28} However, graphene materials converted from these wastes are mostly of low quality with large fractions of defects, contamination, and oxidation.²⁹ These problems are likely to limit the large-scale use of waste materials by the graphene industry.

Recently, the flash Joule heating (FJH) technology, requiring the use of electricity only, has been developed to produce high-quality flash graphene (FG) from various waste materials.^{30,31} With an ultra-high temperature ($\sim 3,000$ K) driven by the local current in the carbon precursor, this technology can force carbon-carbon bonds to break and rearrange for the FG preparation. The FJH technology seems to offer some environmental benefits. It does not use toxic chemicals and provides a new valorization route for various wastes, most of which are landfilled or littered.³² However, to what extent FG produced by the FJH technology is more environmentally sustainable than traditional graphene remains unclear. Its production relies on the use of electricity, which is a major source of CO_2 emissions and air pollution given the use of fossil fuels in many countries such as China.³³ The FG production process releases air pollutants such as CO and C_2H_4 that, if not adequately captured, can affect human health.³⁴ The production, collection, and transportation of feedstocks also have environmental impacts.³⁵ Thus, determining the relative environmental performance of FG produced by the FJH technology requires rigorous quantification using systems approaches like life cycle assessment (LCA).³⁵

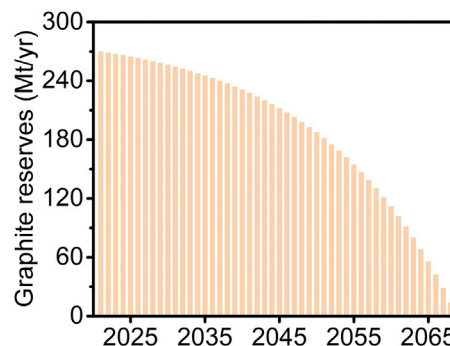


Figure 1. Estimates of global graphite reserves from 2021 to 2068

The natural graphite reserves are currently estimated at 260 million tonnes.

Here we fill the knowledge gap by carrying out an experiment to examine the life cycle environmental impacts of FJH technology.³⁵ We designed an FJH system, based on a continuous alternating current flash Joule heating (AC-FJH) process and a subsequent direct current flash Joule heating (DC-FJH) process, to produce FG from forestry and agricultural residues (i.e., sawdust, wheat straw, corn straw, and rice straw). The experimental results show that about 0.02 g of FGs can be produced from 0.2 g of biomass waste. We also measured the material use, energy consumption, and air emissions of the two processes. The measured data were then fed into an LCA model, with upstream data on feedstock and energy production collected from China. We compared the life cycle impact results with those of the conventional technologies (e.g., oxidation-reduction and electrochemical exfoliation) based on the production of 1 g graphene (as the functional unit).¹⁹ We found that FG produced from biomass waste and by the FJH technology has considerably lower environmental footprints than conventional graphene, particularly the reduction of carbon emissions and freshwater withdrawals by at least 10 times. Notably, our proposed biomasswaste-derived FG could readily become carbon neutral when the FJH process is powered by renewable energy. In addition, the biomasswaste-based FJH technology is much more efficient, with the cost of FG estimated to be one-fifth or even less than that of conventional graphene. Overall, our study reveals that the FJH technology can contribute greatly to the environmental and economic sustainability of graphene production, with the potential to facilitate the transition of circular bioeconomy by valorizing biomass waste.

RESULTS

Flash graphene from four biomass waste sources

As shown in Figure S1 and Table S1, the AC-FJH and DC-FJH devices were fabricated to prepare FG from sawdust, wheat straw, corn straw, and rice straw (Table S2).^{30,31} First, preliminary FG was synthesized in the AC-FJH process, as reflected in the mean Raman spectroscopy (Figure 2A). The biomass-derived preliminary FGs had a high intensity of D band ($\sim 1,350$ cm^{-1}), which implied the presence of a large amount of amorphous or disordered carbon.³⁶ Then, the preliminary FG was further subjected to the DC-FJH process to obtain

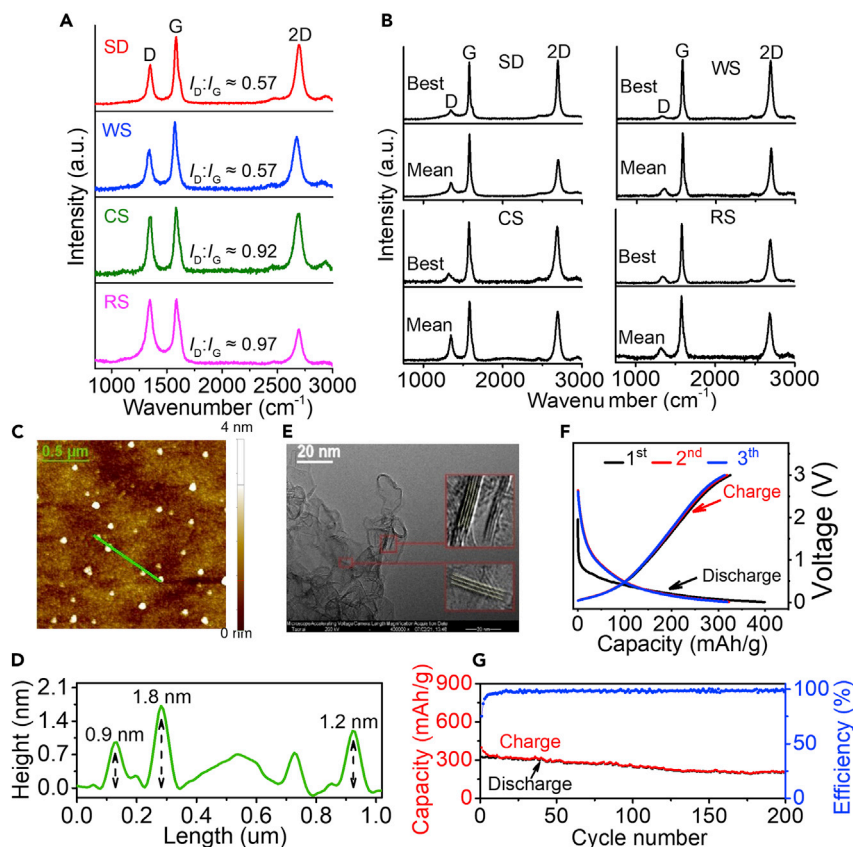


Figure 2. Characteristics and electrochemical performance of various biomass-derived flash graphene (FG)

(A) Raman spectra for various biomass-derived preliminary FG from the AC-FJH process. (B) Raman spectra (best and mean spectra) of FG derived from sawdust (SD), wheat straw (WS), corn straw (CS), and rice straw (RS), respectively. (C) AFM of FG from SD. (D) Height profile along the dotted green line. (E) TEM image of FG from SD. (F) Galvanostatic charge/discharge (GCD) and (G) cycling performances and Coulomb efficiency of FG from SD.

Process inputs and outputs

The yields of preliminary FG from the AC-FJH process were less than 20% (Table S3), owing to the carbon content and thermal stability of the parent materials.^{30,31} The as-prepared preliminary FGs had similar element compositions, including high carbon (82.1%–89.3%), medium oxygen (7.21%–10.6%), and low hydrogen ($\leq 0.94\%$), nitrogen ($\leq 0.65\%$), and sulfur ($\leq 0.24\%$) content (Table S3). In addition, large amounts of bio-gas and oil were produced instantly in the thermal decomposition of biomass ($\sim 2,500$ K, Figure S11), with a total yield of up to 80% (Figure 3A). As shown in Figure 3B

and Table S4, the bio-gas (wt % and vol %) from the various biomass sources was mainly composed of small-molecule gases (such as H₂, CO, CO₂, CH₄, C₂H₂, and C₂H₄). These gases were mainly produced by high-temperature thermal cracking of biomass or bio-oil.^{46,47} The differences in bio-gas content may be caused by biomass components.

In the DC-FJH process, the ultra-high flash temperature ($\sim 3,100$ K, Figure S12) accelerated the sublimation of non-carbon elements. Due to the higher carbon content in its parent material, the yields of FGs in the DC-FJH process were much higher than preliminary FGs in the AC-FJH process, reaching more than 52.5% (Table S3). The carbon content in FGs was significantly increased to more than 90.1%, while the content of other elements (such as oxygen, hydrogen, nitrogen, and sulfur) decreased (Table S3). Figure 3C shows that the process generated 9.88, 6.56, 8.94, and 6.95 g CO₂e of greenhouse gas (GHG) emissions (mainly CO₂ and CH₄) to synthesize 1 g of FG with sawdust, wheat straw, corn straw, and rice straw as raw materials, respectively. Notably, the AC-FJH process was the main source of GHG emissions. The estimated yields of H₂ derived from sawdust, wheat straw, corn straw, and rice straw per gram of FG produced were 0.26, 0.29, 0.36, and 0.31 g, respectively, and the estimated yields of CO were 4.79, 4.72, 5.69, and 5.38 g (Figure 3C).

Compared with preliminary FGs and other reported graphene preparation methods,^{37–40} the final FGs produced from the DC-FJH process had a low-intensity D peak in both the best and mean Raman spectra, indicating the absence of considerable defects (Figure 2B). The intensity ratio of the 2D and G bands demonstrated that the FGs consisted mainly of few-layered graphene structures,⁴¹ which can be further confirmed by the atomic force microscopy (AFM) and transmission electron microscopy (TEM) results (Figures 2C–2E, S5, and S6 and Note S1). More information on assessing FG quality and type, including Raman spectra, AFM, HR-TEM, scanning electron microscopy (SEM), X-ray diffraction (XRD), X-ray photoelectron spectroscopy (XPS), BET surface areas, and pore sizes are provided as supporting information (Note S1 and Figures S5, S6, S7, S8, S9 and S10). Furthermore, the thermal and electrical conductivity of FG at room temperature was 143.5 W/mK and 235 S/cm, respectively, falling within the range for some reported graphene produced by conventional technologies (46.1–187 W/mK and 5.2–276.8 S/cm).^{42–45} Thus, the FG showed good applicability in electrochemical energy storage devices, especially as electrode material in the Li-ion battery (see Figures 2F and 2G and Note S2). These results demonstrated the successful synthesis of high-quality FG from various types of biomass waste.

Total electricity used through the AC-FJH and DC-FJH processes was 0.019, 0.009, 0.017, and 0.018 kWh per g of FG produced from the four biomass sources (sawdust, wheat straw, corn straw, and rice straw; Figure S13 and Note S3).

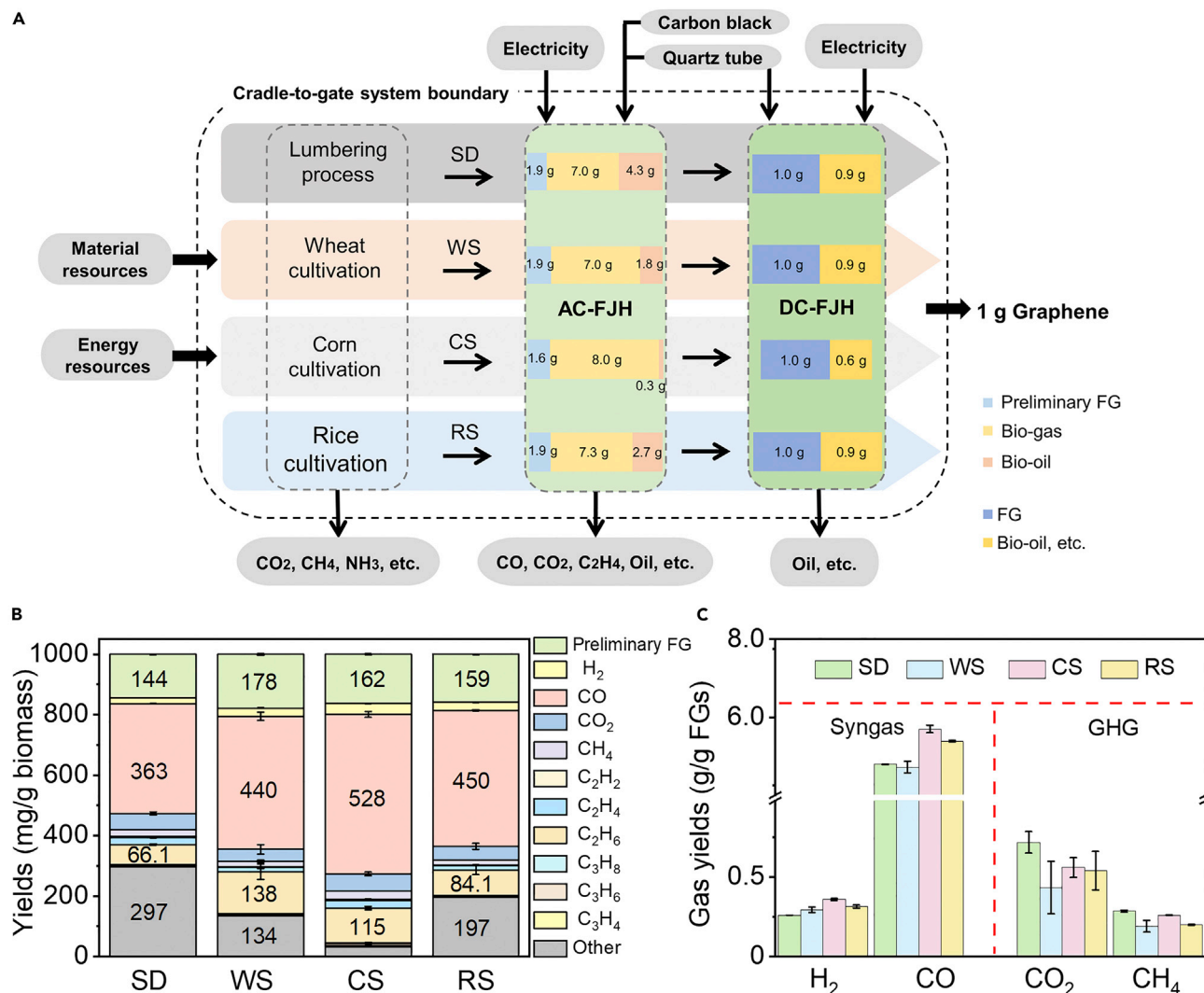


Figure 3. Preparation routes and process of biomass-derived FG

(A) The system boundary for LCA of biomass-based FG systems. The produced bio-gas and bio-oil can be collected and used for fossil fuel substitution, which was described in the [potential offset benefits](#) section.

(B) Yields of each component from SD, WS, CS, and RS in the AC-FJH process, respectively (the other represents bio-oil and uncertain gases). The error bars represent the standard deviation where N = 3.

(C) The yields of syngas and GHG in the synthesis of unit mass net FG from biomass. A more detailed gas composition (vol %) can be found in [Table S6](#).

The differences in electricity use may be related to sample resistance and composition ([Table S5](#)). The AC-FJH and DC-FJH processes at the lab scale were completed in the quartz tube. Each quartz tube weighed about 1 g. Based on our experiment, the tubes needed to be replaced after about 300 cycles due to wear and tear created by the FJH processes. Therefore, the amount of quartz tube consumed to produce 1 g of FG for the four biomass-based FG systems was estimated to be 0.15 g. Considering that quartz tubes can be recycled for reprocessing, their consumption may be reduced during large-scale FGs production.

Climate change impact

The climate change impact pertaining to 1 g of FG production from the four biomass feedstocks based on the ReCiPe 2008

method is presented in [Table S6](#). These results are compared with three traditional graphene production technologies, i.e., electrochemical exfoliation of graphite (EE), chemical oxidation and subsequent chemical reduction (rGO2C), and chemical oxidation and subsequent thermal reduction (rGO2T) ([Figure 4A](#)). The life cycle inventory data for the three graphene production technologies at both the lab scale and a likely commercial scale are from a recent, comprehensive study ([Tables S7 and S8](#)).¹⁹ We recalculated the impact results of these technologies at different scales using the ReCiPe 2008 method instead of the ILCD method ([Tables S9 and S10](#)).

The climate change impact of the four biomass-based FG systems falls in the range of 2.73–11.5 g CO₂e per g of FG produced. These estimates account for the carbon captured in the FG and the fossil fuel offset from the use of bio-gas from the

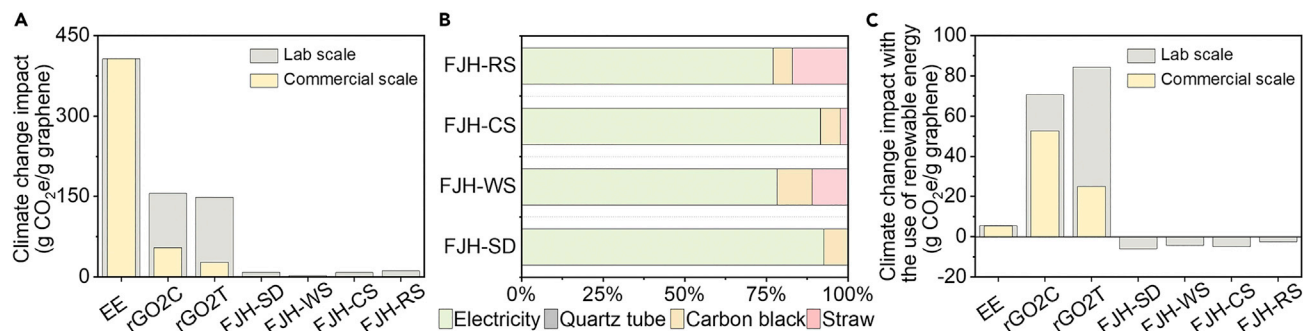


Figure 4. Climate change impact of biomass-based FG systems and conventional graphene systems before and after the use of renewable energy

(A) Comparison of life cycle GHG emissions between biomass-based FG systems and traditional technologies at the lab and commercial scales.

(B) Contribution analysis of the GHG emissions derived from 1 g of FG produced by the four biomass-based FG systems in terms of material and energy inputs.

(C) Comparison of life cycle GHG emissions between biomass-based FG systems and traditional technologies with the use of renewable energy at the lab and commercial scales. EE: electrochemical exfoliation of graphite; rGO2C: chemical oxidation and subsequent chemical reduction; rGO2T: chemical oxidation and subsequent thermal reduction.

FJH processes. They are much lower than the climate change impact of graphene produced by traditional technologies (149–407 g CO₂e at the lab scale and 28–407 g CO₂e at the commercial scale, respectively). This is mainly because the FJH processes require much lower use of electricity and chemical materials. For instance, the electrochemical exfoliation of graphite requires 0.514 kWh of electricity at the lab scale to produce 1 g of graphene, more than 26 times higher than the FJH technology using biomass waste in this study. In addition, the chemical materials, such as calcium hydroxide and hydrazine, required by the chemical oxidation and subsequent chemical reduction technologies also incur substantial GHG emissions, contributing ~27.2% to the total climate change impact. Though most of the traditional technologies could benefit from the likely scale-up scenarios,¹⁹ their climate change impact is still much higher than that of the FJH technology in this study.

Our contribution analysis indicates that in the case of China, electricity is the main driver of the climate change impact of biomass-based FG systems (Figure 4B), accounting for 77.1%–92.6% of total emissions. If the electricity system is decarbonized with the use of renewable energy, all four biomass-based FG systems could achieve carbon-neutral or even carbon-negative values when considering the fossil fuel offset options (see the [potential offset benefits](#) of the [experimental procedures](#) section for assumptions) (–2.53 to –5.96 g CO₂e per g of FG; Figure 4C). This could be achieved when the industry itself adopts renewable energy on site without the use of grid electricity (a more aggressive mitigation scenario) or when the grid systems become greener with increasing penetration of renewables (a more passive mitigation scenario). By contrast, even when the electricity system is decarbonized, the traditional graphene production technologies would still contribute to climate change (~5.53–84.3 g CO₂e at the lab scale and ~5.41–52.6 g CO₂e per g of FG on the likely commercial scale). This is due to the intensive use of chemical materials, the production of which incurs direct process GHG emissions that are difficult to abate. For the biomass-based FG systems, carbon black and straw production phases contribute 5.89%–10.7% and 2.37%–17.0% to the total climate change impact, respectively. Quartz tubes consumed during the

AC-FJH and DC-FJH processes make negligible contributions (less than 0.1%).

Other environmental impacts

In addition to the climate change impact, we evaluated a set of other environmental impacts that are relevant to biomass-derived product systems (see [experimental procedures](#)). The biomass-based FG systems have much smaller impacts than the three traditional technologies across all impact categories evaluated (Figure 5). The fossil depletion impact is estimated to be 1.81 to 3.97 g oil-eq (Table S6), only 1.78%–7.65% of that of traditional technologies at the lab scale (43.8–102 g oil-eq). The terrestrial acidification impact amounts to 0.02–0.04 g SO₂-eq, about 1.88%–7.50% that of traditional technologies (0.57–1.13 g SO₂-eq). The freshwater eutrophication impact shows a negative value due to the offset benefits from fossil fuel substitution, –3.18 to –0.40 mg P-eq, whereas it is 1.92–26.5 mg P-eq for traditional technologies. The metal depletion impact falls in the range of 0.08–0.13 g Fe-eq, representing 0.08%–5.32% that of traditional technologies (2.40–104 g Fe-eq). The particulate matter formation impact amounts to 0.00–0.01 g PM10-eq, about 0.57%–6.89% that of traditional technologies (0.19–0.44 g PM10-eq). The photochemical oxidant formation impact is estimated to be 0.90–26.7 mg NMVOC-eq, about 0.10%–9.62% that of traditional technologies (0.28–0.91 g NMVOC-eq). The water depletion impact falls in the range of –1.31 to 2.25 kg water, much lower than that of traditional technologies (29.8–317 kg water). The new FJH technology also has much smaller impacts than the three traditional technologies at the likely commercial scale (Figure S14).

Similar to the climate change impact, electricity use during the AC-FJH and DC-FJH processes has the largest contribution to most of the environmental impact categories evaluated, i.e., fossil depletion (61.8%–77.6%), terrestrial acidification (66.8%–87.4%), metal depletion (34.4%–64.5%), particulate matter formation (72.0%–87.2%), and photochemical oxidant formation (79.8%–90.9%) (Figure S15). The straw production phase makes the largest contribution to freshwater eutrophication for the FG systems based on wheat straw and rice straw (61.9% and

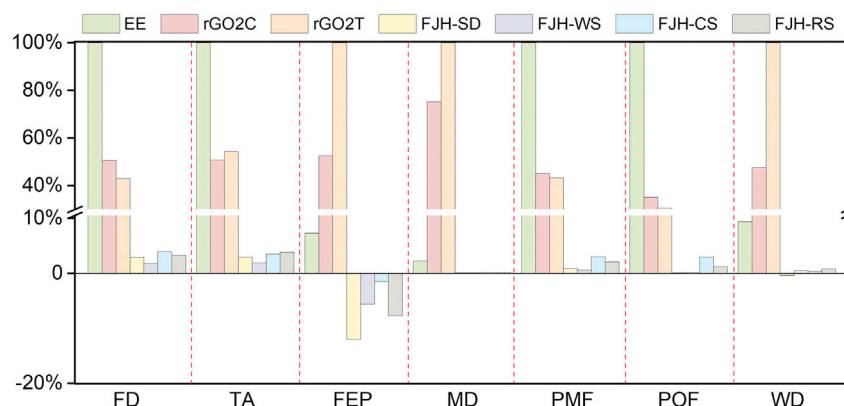


Figure 5. Other life cycle environmental impacts of biomass-based FG systems and conventional graphene systems at the lab scale are based on the ReCiPe 2008 method

For each impact category, the highest impact value is set to be 100%, and the value of other technologies equals to be the percentage shares of each product system based on this highest impact. FD: fossil depletion; TA: terrestrial acidification; FEP: freshwater eutrophication; MD: metal depletion; PMF: particulate matter formation; POF: photochemical oxidant formation; WD: water depletion.

66.5%, respectively) due to the application of nitrogen fertilizer during crop production. It also makes the largest contribution to water depletion for the FG systems based on wheat straw, corn straw, and rice straw (52.9%–79.1%) due to crop irrigation water use (Table S11). Carbon black is the main contributor to freshwater eutrophication for the sawdust- and corn straw-based FG systems (94.9% and 56.2%, respectively) and to water depletion for the sawdust-based FG system (91.0%) because of its relatively higher freshwater eutrophication and water depletion impacts during the upstream production processes.

Among the four biomass-based FG systems, the wheat straw-based FG system performs the best across most environmental impacts, including climate change, fossil fuel depletion, terrestrial acidification, metal depletion, and particulate matter formation (Table S6). This is mainly because it requires the least amount of electricity (0.009 kWh per 1 g of graphene) during the AC-FJH and DC-FJH processes, only about half of that consumed by the other three biomass-based FG systems. The wheat straw-based FG system performs better than the rice straw-based FG system for water depletion because of the intensive use of irrigation water in rice production.

DISCUSSION

Our study has demonstrated that the FG produced from biomass waste based on the new FJH technology has substantially lower environmental impacts than graphene produced by traditional production technologies. Notably, FG has a substantially lower carbon footprint and could easily become carbon neutral when renewable energy is used. In comparison, it would be more difficult for traditional graphene production technologies to achieve carbon neutrality partly because of the intensive use of chemical materials. The chemical industry faces a great challenge to be decarbonized for heavy capital investment, complex processes, and emissions from non-energy sources.⁴⁸ The lower impacts of FG depend partly on the utilization of processed bio-gas to produce energy and displace fossil fuels. In the future when fossil fuels are replaced by renewables, the process bio-gas can still be utilized to produce electricity⁴⁹ as an input to the FG production processes, reducing the reliance on external electricity supply. Although our data are primarily from China, our findings are likely of global relevance. Additional analysis based on other

countries' electricity and biomass data shows that FG consistently outperforms graphene produced from traditional technologies (Table S12), suggesting its potential to contribute to the environmental sustainability of the graphene industry on a global scale.

Our use of laboratory data, albeit at the experimental scale, offers insight into the potential impact of the FJH technology when it is industrialized. By our estimation, an automated device can produce FG in only 5 s, and its production capacity can reach 10 kg/day if working continuously (Figure S16). As with the traditional technologies,¹⁹ industrial-scale FJH devices (e.g., through automation) will be more energy and material efficient than lab-scale FJH devices, and a reduction in life cycle impacts by at least 40% is expected. It is worth noting that the FG itself can be used as the conductive additive, but we found that it would decrease production efficiency and increase the environmental impacts of FG production. For example, the climate change impact of the sawdust-based FG system would increase from 8.88 to 22.7 g CO₂e/g of FG. Therefore, we recommend using carbon black, instead of FG itself, as the conductive additive for FG production. Future research could explore cheaper and more environmentally friendly alternatives to carbon black to further lower the environmental impacts of FG.

There are some uncertainties associated with our life cycle modeling, but they are unlikely to affect the relative performance of traditional graphene and new few-layered graphene production technologies in China as estimated by our life cycle analysis. Electricity is the primary contributor in most impact categories for the FG production system, and its use intensity—with only a small uncertainty as shown by our experiment—is much smaller than that in the conventional graphene systems. Biomass production can be a primary contributor to the freshwater eutrophication and water depletion impacts of FG (Figures S15B and S15G). This life cycle phase poses some uncertainty given the large spatial variability of agricultural systems due in part to the influence of local climate and soil.^{50,51} In our analysis, the life cycle estimates for FG were based on national average data. At the regional level, freshwater eutrophication impact varies from −3.18 to −0.28 mg P-eq per g of graphene produced; even the upper bound is still much lower than that of graphene produced by the three traditional technologies (1.92–26.5 mg P-eq). The same goes for the water depletion impact (Figure S17). Therefore, despite these uncertainties, we expect our broad conclusion regarding the lower

environmental impacts of FG to hold robustly. One limitation of our life cycle modeling is the exclusion of biomass transportation because this phase contributes negligible (<0.5%) to all the considered impact categories (assuming a distance of 50 km, available at Zenodo: <https://doi.org/10.5281/zenodo.7314781>).⁵² However, transportation may become a hotspot of environmental impacts if the FG industry becomes globalized and biomass is transported over long distances. In such a case, it needs to be considered.

The FJH technology might provide additional benefits along the upstream and downstream supply chain. On the upstream side, it provides a new and profitable route of valorization for biomass waste. Our analysis indicates that converting biomass to FG could be 600–850 times more profitable than converting them into biochar and bioenergy (Table S13). Thus, the new technology can help facilitate the collection and utilization of biomass waste, contributing to the development of circular bioeconomy. On the downstream side, the cost of conventional graphenes, such as graphene oxide, is high (about \$50–990 per kg),⁵³ limiting its potential applications in only high-tech sectors such as supercomputers and liquid crystal display materials. By contrast, the cost of producing 1 kg of biomass waste-derived FG is estimated at \$5.41–8.84 per kg (including materials, labor, depreciation, maintenance, and energy costs; Table S13). The much lower cost of biomass waste-derived FG—which is expected to drop further at the commercial scale—could help promote its broad use in many other industries such as building.^{54,55} These benefits of biomass-based FG in upstream and downstream applications can be a focus of future research.

EXPERIMENTAL PROCEDURES

Resource availability

Lead contact

Further information and requests should be directed to and will be fulfilled by the lead contact, Yi Yang (yi.yang@cqu.edu.cn).

Materials availability

Material generated in this study will be made available on request, but we may require a payment and/or a completed materials transfer agreement if there is potential for commercial application.

Data and code availability

All data needed to evaluate the conclusions in the paper are present in the paper and/or the supplemental information. The detailed data and calculation for the main LCA results of this study are provided at Zenodo: <https://doi.org/10.5281/zenodo.7314781>.

Synthesis of high-quality flash graphene

To produce high-quality FG, various biomass sources (including sawdust, wheat straw, corn straw, and rice straw) containing 5 wt % carbon black (Super p li, Lizhiyuan, China) were treated as a conductive by using AC-FJH and DC-FJH devices (Figure S1 and Table S1). Briefly, the biomass waste was crushed into powder (80 mesh) and dried to constant weight, followed by grinding with carbon black in a mortar. Then, 0.2 g of the mixture was loaded in a quartz tube (tube thickness: 2 mm, inner diameter: 6 mm, length: 45 mm) and pressed tightly with copper electrodes at each end to obtain a low resistivity. The mixture was then placed in a vacuum desiccator (~0.6 psi) and operated on alternating current (200 V, 50 Hz) for ~6 s to release the necessary volatiles and produce preliminary FG. A large amount of bio-gas was produced from the mixture in the AC-FJH process. Therefore, one end of the copper electrode was hollow to facilitate the collection of the generated gas with a gas bag (200 mL). Subsequently, 0.2 g of preliminary FG was subjected to DC-FJH to obtain high-quality FG at the desired discharge voltage and time.

Characterizations

Raman spectra was carried out using a XploRA Raman spectrometer with a 532-nm (5-mW) laser source under a 50× objective microscope. And the Raman parameters were fitted with three distinctive Lorentz peaks using Lab-Spec6.4 software, corresponding to G (~1,580 cm⁻¹), D (~1,350 cm⁻¹), and 2D (~2,700 cm⁻¹) bands, respectively. XRD of FGs derived from various biomass was performed using rigaku Ultima IV with Cu K α radiation at 40 kV, 40 mA in the 2 θ range of 5°–80°. XPS of FG was examined by using Thermo ESCALAB 250 XI with Al K α X-ray radiation (400 μ m spot size) at a base pressure of 10⁻⁸ to 10⁻¹⁰ mbar. Survey scans were acquired with a pass energy of 50 eV and a step size of 0.05 eV. Elemental spectra of FGs were acquired with a pass energy of 30 eV and a step size of 0.1 eV. The binding energies of high resolutions spectra were calibrated at C 1s of 284.6 eV. N₂ adsorption/desorption isotherms of FG were conducted on a Quantachrome Autosorb iQ2 instrument at 77 K after degassing at 573 K for 8 h. Specific surface area (S_{BET}) and total pore volume (V_{T}) were determined by the BET equation. The C/H/N/S analysis of FGs was performed using an elemental analyzer (Vario EL III, Germany). The morphologies of FGs were acquired by using scanning electron microscopy (SEM, ZEISS Gemini 300) and TEM (Tecnai G2 F20 S-Twin, FEI). The flake images of FG were determined using an AFM (Asylum Research MFP-3D, USA). The thermal property of FG was measured by a Hot Disk thermal constant analyzer (Hot Disk TPS2500S, Sweden). The electrical conductivity of FG was measured by the four-point probe technique (YAOS FM1-00GH, China).

The collected bio-gas compositions were quantitatively analyzed by gas chromatography (GC-960, Haixin, China) equipped with a thermal conductivity detector channel to test H₂, CO, CO₂, and CH₄. For H₂, the carrier gas was N₂, and the temperatures of the injector, detector, and oven were 393, 383, and 393 K, respectively; while for testing CO, CO₂, and CH₄, the carrier gas was changed to He, and other conditions were the same. A standard gas mixture of the above gases in N₂ was purchased from Air Liquide Compressed Gas (China). Hydrocarbons (such as C₂H₂, C₂H₄, C₂H₆, C₃H₈, C₃H₆, C₃H₄, and C₄H₁₀) were checked on a flame-ionization detector with N₂ as the carrier gas and an oven temperature of 393 K. A standard gas mixture of these hydrocarbons was also purchased from Air Liquide Compressed Gas (China). The response factor was obtained using standard gases for quantitative analysis.

The electrochemical performance of FG was performed using a CR2032 cell. The FG was directly used as the anodic, while Li metal, Celgard K2045, and 1 M lithium hexafluorophosphate dissolved in 1:1:1 ethylene carbonate:dimethyl carbonate:diethyl carbonate as the counter electrode, separator, and electrolyte, respectively. The anodic was prepared with 80 wt % of FG, 10 wt % acetylene black, and 10 wt % polyvinylidene difluoride in N-methyl-2-pyrrolidone. The well-mixed electrode material was then pasted onto Cu foil and dried at 85°C in a vacuum oven. All the cells were assembled in a glove box under an argon atmosphere and stabilized to an equilibrium state for about 8 h. The galvanostatic charge/discharge curves of the cells were recorded by a Battery Testing System (LANHE, CT2001A, China) in a voltage range of 0.01–3.0 V (vs. Li+/Li) for the anode. The cyclic voltammetry test and the electrochemical impedance spectroscopy test were carried out on an electrochemical workstation (CHI-660E).

Life cycle assessment

LCA is a systematic approach to evaluating the potential environmental impacts associated with a product or service throughout its entire life cycle, i.e., from raw material extraction, processing, manufacturing, and use to final disposal.^{35,56,57} In this section, we provide a detailed description of the goal and scope definition, inventory analysis, and impact assessment of our LCA following ISO guidelines.³⁵

Goal and scope definition

The goal of this LCA study was to evaluate the environmental impacts of biomass-derived FG production from cradle to gate and to compare with life cycle results of the conventional graphene production technologies in China. As shown in Figure 3A, the system boundary of the FG production covers the three main phases: biomass cultivation, AC-FJH, and DC-FJH processes. Since the transportation of different materials from the manufacturing location to the laboratory is not included in Cossutta et al.,¹⁹ we did not consider the

transportation of biomass and quartz tube in this study either to keep the same system boundary and the results comparable. In general, transportation makes a small contribution in biomass systems (data given in Zenodo: <https://doi.org/10.5281/zenodo.7314781>). The functional unit of our LCA is one g of FG produced, which serves as the basis for comparison³⁵ with the conventional technologies.

Inventory analysis

We relied on both experimental data and LCA literature or databases to estimate the life cycle environmental impacts of FG production. The direct material and energy inputs and emissions during the FG production were measured in our experiment (see Table S14). As for data quality requirements, several experiments were conducted, and the errors in the yield ratio of FG and gas concentration were all within 2%, respectively. Data for crop cultivation—including usage of pesticides, fertilizers, and diesel—were collected at the province level and from relevant literature and statistical yearbooks (details available in Table S11). Various types of emissions could be produced from the use of these inputs and were estimated using emission factors following the methods created in previous studies.⁵⁸ The overall environmental impacts derived from crop cultivation were allocated to the straw according to its market values. Specifically, 12.8%, 8.01%, and 13.9% of total environmental impacts of wheat, corn, and rice cultivation were allocated to wheat straw, corn straw, and rice straw, respectively. The environmental impacts associated with sawdust production were neglected in this study because it is residue from the wood processing industry and is usually considered waste that has zero emission burdens.^{59,60} In terms of renewable energy for decarbonizing FG production, hydroelectricity was assumed to be used because hydropower accounts for the largest proportion of China's renewable electricity generation currently.⁶¹ As stated before, the life cycle inventory data for the three conventional graphene production technologies at both the lab scale and the likely commercial scale are from Cossutta et al.¹⁹ with no adjustments. Data on the life cycle burdens of energy, agricultural inputs, and other materials (e.g., electricity, fertilizers, carbon black, and quartz tube) were obtained from the Ecoinvent 3.5 database and the PE International database under the Gabi 8 platform (the Cut-off System Model).⁶²

Impact assessment

In the life cycle impact assessment (LCIA) phase, inventory results are translated to environmental impact potentials to understand their relative environmental significance. The LCIA model used in our study is the ReCiPe 2008 method.⁶³ As listed in Table S6, the considered impact categories include climate change, fossil depletion, terrestrial acidification, freshwater eutrophication, metal depletion, particulate matter formation, photochemical oxidant formation, and water depletion, and all the impacts are expressed based on the functional unit. Due to the lack of pesticide-related data during the biomass cultivation process, the toxicity impact categories are not considered in this study.⁶⁴

Potential offset benefits

Since a large amount of bio-gas and oil is produced during the AC-FJH process, they can be collected and utilized to displace fossil fuels. The bio-gas can substitute for coke oven gas and the bio-oil can be used as an alternative for coal tar produced as a by-product of coke production.⁶⁵ Detailed data are provided in Table S15. Note that we followed Hill et al.⁶⁶ and applied a 1:0.5 instead of 1:1 displacement ratio, i.e., 1 MJ of bioenergy displaces only 0.5 MJ of fossil fuels, given the potential rebound effect associated with the additional bioenergy as shown by a large body of studies.^{64,67} Then the total environmental impacts of FG production are the life cycle environmental impacts derived from the energy and materials inputs subtracting the offset benefits through the substitution of fossil fuels.

SUPPLEMENTAL INFORMATION

Supplemental information can be found online at <https://doi.org/10.1016/j.oneear.2022.11.006>.

ACKNOWLEDGMENTS

This work was supported by funds from the Yangtze delta region healthy agriculture institute.

AUTHOR CONTRIBUTIONS

X.Z. and Y.Y. conceived the research; most experimental work (FG preparation, characterizations, and application and bio-gas analysis) was performed by C.J., assisted by Y.L., F.Y., L.L., L.S., T.T., X.W., Z.H., J.G., J.L., T.W., L.W., T.B., and M.W.; M.P. developed the models and conducted the simulations, assisted by Y.L., M.Z., B.L., L.F., X.Y., and L.Z.; X.Z., Y.Y., S.Z., F.Y., G.L., and Y.Z. analyzed the results; C.J., M.P., X.Z., Y.Y., F.Y., and Y.Z. wrote the manuscript. All authors reviewed the final manuscript.

DECLARATION OF INTERESTS

The authors declare no competing interests.

Received: April 6, 2022

Revised: May 3, 2022

Accepted: November 18, 2022

Published: December 16, 2022

REFERENCES

- Geim, A.K., and Novoselov, K.S. (2007). The rise of graphene. *Nat. Mater.* 6, 183–191.
- Stoller, M.D., Park, S., Zhu, Y., An, J., and Ruoff, R.S. (2008). Graphene-based ultracapacitors. *Nano Lett.* 8, 3498–3502.
- Dreyer, D.R., Todd, A.D., and Bielawski, C.W. (2014). Harnessing the chemistry of graphene oxide. *Chem. Soc. Rev.* 43, 5288–5301.
- Li, X., Yu, J., Wageh, S., Al-Ghamdi, A.A., and Xie, J. (2016). Graphene in photocatalysis: a review. *Small* 12, 6640–6696.
- Wang, Y., Li, X., Jiang, Z., Tong, L., Deng, W., Gao, X., Huang, X., Zhou, H., Yu, Y., Ye, L., et al. (2021). Ultrahigh-speed graphene-based optical coherent receiver. *Nat. Commun.* 12, 5076.
- Kemp, K.C., Seema, H., Saleh, M., Le, N.H., Mahesh, K., Chandra, V., and Kim, K.S. (2013). Environmental applications using graphene composites: water remediation and gas adsorption. *Nanoscale* 5, 3149–3171.
- Radich, E.J., and Kamat, P.V. (2012). Origin of reduced graphene oxide enhancements in electrochemical energy storage. *ACS Catal.* 2, 807–816.
- Li, Y., Liu, X., Tan, L., Cui, Z., Yang, X., Zheng, Y., Yeung, K.W.K., Chu, P.K., and Wu, S. (2018). Rapid sterilization and accelerated wound healing using Zn²⁺ and graphene oxide modified g-C₃N₄ under dual light irradiation. *Adv. Funct. Mater.* 28, 1800299.
- Arvidsson, R., Boholm, M., Johansson, M., and de Montoya, M.L. (2018). “Just carbon”: ideas about graphene risks by graphene researchers and innovation advisors. *Nanoethics* 12, 199–210.
- Jianchao, H., Tongning, M., and Pingkuo, L. (2019). Comprehensive evaluation on graphene's potentials and industrial development in China. *Resour. Policy* 63, 101446.
- Moon, J.Y., Kim, M., Kim, S.I., Xu, S., Choi, J.H., Whang, D., Watanabe, K., Taniguchi, T., Park, D.S., Seo, J., et al. (2020). Layer-engineered large-area exfoliation of graphene. *Sci. Adv.* 6, eabc6601.
- Voiry, D., Yang, J., Kupferberg, J., Fullon, R., Lee, C., Jeong, H.Y., Shin, H.S., and Chhowalla, M. (2016). High-quality graphene via microwave reduction of solution-exfoliated graphene oxide. *Science* 353, 1413–1416.
- Parvez, K., Wu, Z.S., Li, R., Liu, X., Graf, R., Feng, X., and Müllen, K. (2014). Exfoliation of graphite into graphene in aqueous solutions of inorganic salts. *J. Am. Chem. Soc.* 136, 6083–6091.
- Saha, S., Lakhe, P., Mason, M.J., Coleman, B.J., Arole, K., Zhao, X., Yakovlev, S., Uppili, S., Green, M.J., and Hule, R.A. (2021). Sustainable production of graphene from petroleum coke using electrochemical exfoliation. *npj 2D Mater. Appl.* 5, 75.
- Choucair, M., Thordarson, P., and Stride, J.A. (2009). Gram-scale production of graphene based on solvothermal synthesis and sonication. *Nat. Nanotechnol.* 4, 30–33.
- Matsumoto, M., Saito, Y., Park, C., Fukushima, T., and Aida, T. (2015). Ultrahigh-throughput exfoliation of graphite into pristine ‘single-layer’

- graphene using microwaves and molecularly engineered ionic liquids. *Nat. Chem.* **7**, 730–736.
17. Yang, S., Brüller, S., Wu, Z.S., Liu, Z., Parvez, K., Dong, R., Richard, F., Samori, P., Feng, X., and Müllen, K. (2015). Organic radical-assisted electrochemical exfoliation for the scalable production of high-quality graphene. *J. Am. Chem. Soc.* **137**, 13927–13932.
 18. Ye, R., and Tour, J.M. (2019). Graphene at fifteen. *ACS Nano* **13**, 10872–10878.
 19. Cossutta, M., McKechnie, J., and Pickering, S.J. (2017). A comparative LCA of different graphene production routes. *Green Chem.* **19**, 5874–5884.
 20. Mayyas, A., Steward, D., and Mann, M. (2019). The case for recycling: overview and challenges in the material supply chain for automotive lithium-ion batteries. *Sustain. Mater. Technol.* **19**, e00087.
 21. Zinke, R., and Werkheiser, W. (2018). Mineral Commodity Summaries 2018 (US Geological Survey), p. 200.
 22. Mining Review Africa (2021). Natural Graphite Production Expected to Grow by 7.6% in 2021. <https://www.miningreview.com/battery-metals/natural-graphite-production-expected-to-grow-by-7-6-in-2021>.
 23. Zhao, L., Ding, B., Qin, X.-Y., Wang, Z., Lv, W., He, Y.B., Yang, Q.H., and Kang, F. (2022). Revisiting the roles of natural graphite in ongoing lithium-ion batteries. *Adv. Mater.* **34**, 2106704.
 24. Ma, C., Zhao, Y., Li, J., Song, Y., Shi, J., Guo, Q., and Liu, L. (2013). Synthesis and electrochemical properties of artificial graphite as an anode for high-performance lithium-ion batteries. *Carbon* **64**, 553–556.
 25. Nasir, S., Hussein, M.Z., Yusof, N.A., and Zainal, Z. (2017). Oil palm waste-based precursors as a renewable and economical carbon sources for the preparation of reduced graphene oxide from graphene oxide. *Nanomaterials* **7**, 182.
 26. Li, J., Yan, Q., Zhang, X., Zhang, J., and Cai, Z. (2019). Efficient conversion of lignin waste to high value bio-graphene oxide nanomaterials. *Polymers* **11**, 623.
 27. Sun, Z., Zheng, M., Hu, H., Dong, H., Liang, Y., Xiao, Y., Lei, B., and Liu, Y. (2018). From biomass wastes to vertically aligned graphene nanosheet arrays: a catalyst-free synthetic strategy towards high-quality graphene for electrochemical energy storage. *Chem. Eng. J.* **336**, 550–561.
 28. Kong, X., Zhu, Y., Lei, H., Wang, C., Zhao, Y., Huo, E., Lin, X., Zhang, Q., Qian, M., Mateo, W., et al. (2020). Synthesis of graphene-like carbon from biomass pyrolysis and its applications. *Chem. Eng. J.* **399**, 125808.
 29. Munuera, J., Britnell, L., Santoro, C., Cuéllar-Franca, R., and Casiraghi, C. (2021). A review on sustainable production of graphene and related life cycle assessment. *2D Mater.* **9**, 012002.
 30. Luong, D.X., Bets, K.V., Algozeeb, W.A., Stanford, M.G., Kittrell, C., Chen, W., Salvatierra, R.V., Ren, M., McHugh, E.A., Advincula, P.A., et al. (2020). Gram-scale bottom-up flash graphene synthesis. *Nature* **577**, 647–651.
 31. Algozeeb, W.A., Savas, P.E., Luong, D.X., Chen, W., Kittrell, C., Bhat, M., Shahsavari, R., and Tour, J.M. (2020). Flash graphene from plastic waste. *ACS Nano* **14**, 15595–15604.
 32. Chew, K.W., Chia, S.R., Yen, H.W., Nomanbhay, S., Ho, Y.C., and Show, P.L. (2019). Transformation of biomass waste into sustainable organic fertilizers. *Sustainability* **11**, 2266.
 33. Cao, L., Diana, J.S., Keoleian, G.A., and Lai, Q. (2011). Life cycle assessment of Chinese shrimp farming systems targeted for export and domestic sales. *Environ. Sci. Technol.* **45**, 6531–6538.
 34. Huijbregts, M.A.J., Steinmann, Z.J.N., Eishout, P.M.F., Stam, G., Verones, F., Vieira, M., Zijp, M., Hollander, A., and Van Zelm, R. (2017). ReCiPe2016: a harmonised life cycle impact assessment method at midpoint and endpoint level. *Int. J. Life Cycle Assess.* **22**, 138–147.
 35. International Organization for Standardization. ISO 14040: 2006. Environmental Management-Life Cycle Assessment, Principles and Framework; International Organization for Standardization: Geneva, Switzerland.
 36. Wu, J.B., Lin, M.L., Cong, X., Liu, H.N., and Tan, P.H. (2018). Raman spectroscopy of graphene-based materials and its applications in related devices. *Chem. Soc. Rev.* **47**, 1822–1873.
 37. Islam, A., Mukherjee, B., Pandey, K.K., and Keshri, A.K. (2021). Ultra-fast, chemical-free, mass production of high quality exfoliated graphene. *ACS Nano* **15**, 1775–1784.
 38. Voiry, D., Yang, J., Kupferberg, J., Fullon, R., Lee, C., Jeong, H.Y., Shin, H.S., and Chhowalla, M. (2016). High-quality graphene via microwave reduction of solution-exfoliated graphene oxide. *Science* **353**, 1413–1416.
 39. Khan, U., O'Neill, A., Lotya, M., De, S., and Coleman, J.N. (2010). High-concentration solvent exfoliation of graphene. *Small* **6**, 864–871.
 40. Chen, J., Yao, B., Li, C., and Shi, G. (2013). An improved Hummers method for eco-friendly synthesis of graphene oxide. *Carbon* **64**, 225–229.
 41. Chen, Z., Ren, W., Gao, L., Liu, B., Pei, S., and Cheng, H.-M. (2011). Three-dimensional flexible and conductive interconnected graphene networks grown by chemical vapour deposition. *Nat. Mater.* **10**, 424–428.
 42. Hou, Z.L., Song, W.L., Wang, P., Meziani, M.J., Kong, C.Y., Anderson, A., Maimaiti, H., LeCroy, G.E., Qian, H., and Sun, Y.-P. (2014). Flexible graphene-graphene composites of superior thermal and electrical transport properties. *ACS Appl. Mater. Interfaces* **6**, 15026–15032.
 43. Zeng, Y., Li, T., Yao, Y., Li, T., Hu, L., and Marconnet, A. (2019). Thermally conductive reduced graphene oxide thin films for extreme temperature sensors. *Adv. Funct. Mater.* **29**, 1901388.
 44. Luo, D., Zhang, G., Liu, J., and Sun, X. (2011). Evaluation criteria for reduced graphene oxide. *J. Phys. Chem. C* **115**, 11327–11335.
 45. Xu, C., Shi, X., Ji, A., Shi, L., Zhou, C., and Cui, Y. (2015). Fabrication and characteristics of reduced graphene oxide produced with different green reductants. *PLoS One* **10**, e0144842.
 46. Usmani, Z., Sharma, M., Karpichev, Y., Pandey, A., Chander Kuhad, R., Bhat, R., Punia, R., Aghbashlo, M., Tabatabaei, M., and Gupta, V.K. (2020). Advancement in valorization technologies to improve utilization of bio-based waste in bioeconomy context. *Renew. Sustain. Energy Rev.* **131**, 109965.
 47. Yao, D., Wu, C., Yang, H., Zhang, Y., Nahil, M.A., Chen, Y., Williams, P.T., and Chen, H. (2017). Co-production of hydrogen and carbon nanotubes from catalytic pyrolysis of waste plastics on Ni-Fe bimetallic catalyst. *Energy Convers. Manag.* **148**, 692–700.
 48. Gross, S. (2021). The Challenge of Decarbonizing Heavy Industry (Brookings).
 49. Banja, M., Jégard, M., Motola, V., and Sikkema, R. (2019). Support for biogas in the EU electricity sector – a comparative analysis. *Biomass Bioenergy* **128**, 105313.
 50. Liu, B., Gu, W., Yang, Y., Lu, B., Wang, F., Zhang, B., and Bi, J. (2021). Promoting potato as staple food can reduce the carbon-land-water impacts of crops in China. *Nat. Food* **2**, 570–577.
 51. Yang, Y., Pelton, R.E.O., Kim, T., and Smith, T.M. (2020). Effects of spatial scale on life cycle inventory results. *Environ. Sci. Technol.* **54**, 1293–1303. <https://doi.org/10.1021/acs.est.9b03441>.
 52. Wang, C., Zhang, L., Zhou, P., Chang, Y., Zhou, D., Pang, M., and Yin, H. (2019). Assessing the environmental externalities for biomass- and coal-fired electricity generation in China: a supply chain perspective. *J. Environ. Manage.* **246**, 758–767.
 53. He, K., Zhang, Z.Y., and Zhang, F.S. (2021). Synthesis of graphene and recovery of lithium from lithiated graphite of spent Li-ion battery. *Waste Manag.* **124**, 283–292.
 54. Papanikolaou, I., Arena, N., and Al-Tabbaa, A. (2019). Graphene nanoplatelet reinforced concrete for self-sensing structures – a lifecycle assessment perspective. *J. Clean. Prod.* **240**, 118202.
 55. Moreno-Navarro, F., Sol-Sánchez, M., Gámiz, F., and Rubio-Gámez, M. (2018). Mechanical and thermal properties of graphene modified asphalt binders. *Constr. Build. Mater.* **180**, 265–274.
 56. International Organization for Standardization. ISO 14044: 2006. Environmental Management, Life Cycle Assessment, Requirements and Guidelines; International Organization for Standardization: Geneva, Switzerland.

57. Finnveden, G., Hauschild, M.Z., Ekvall, T., Guinée, J., Heijungs, R., Hellweg, S., Koehler, A., Pennington, D., and Suh, S. (2009). Recent developments in life cycle assessment. *J. Environ. Manage.* 91, 1–21.
58. Yang, Y., Bae, J., Kim, J., and Suh, S. (2012). Replacing gasoline with corn ethanol results in significant environmental problem-shifting. *Environ. Sci. Technol.* 46, 3671–3678.
59. Iribarren, D., Moreira, M.T., and Feijoo, G. (2010). Implementing by-product management into the life cycle assessment of the mussel sector. *Resour. Conserv. Recycl.* 54, 1219–1230.
60. Havukainen, J., Nguyen, M.T., Väisänen, S., and Horttanainen, M. (2018). Life cycle assessment of small-scale combined heat and power plant: environmental impacts of different forest biofuels and replacing district heat produced from natural gas. *J. Clean. Prod.* 172, 837–846.
61. Yearbook, C.S. (2022). National bureau of statistics of China. China Statistical Yearbook.v (China Statistics Press).
62. Thinkstep, A. (1992). GaBi Software System and Database for Life Cycle Engineering (LBP–University of Stuttgart).
63. Goedkoop, M., Heijungs, R., Huijbregts, M., De Schryver, A., Struijs, J., and Van Zelm, R. (2009). ReCiPe 2008. A Life Cycle Impact Assessment Method Which Comprises Harmonised Category Indicators at the Midpoint and the Endpoint Level, 1 (RVIM), pp. 1–126. <http://www.lcia-recipe.net/>.
64. Rajagopal, D., and Plevin, R.J. (2013). Implications of market-mediated emissions and uncertainty for biofuel policies. *Energy Pol.* 56, 75–82.
65. Yang, Q., Zhou, H., Bartocci, P., Fantozzi, F., Mašek, O., Agblevor, F.A., Wei, Z., Yang, H., Chen, H., Lu, X., et al. (2021). Prospective contributions of biomass pyrolysis to China's 2050 carbon reduction and renewable energy goals. *Nat. Commun.* 12, 1698.
66. Hill, J., Tajibaeva, L., and Polasky, S. (2016). Climate consequences of low-carbon fuels: the United States renewable fuel standard. *Energy Pol.* 97, 351–353.
67. Yang, Y., and Tilman, D. (2020). Soil and root carbon storage is key to climate benefits of bioenergy crops. *Biofuel Res. J.* 7, 1143–1148.